Electronic Supplementary Information (ESI) for Chemical Communications
This journal is (c) The Royal Society of Chemistry 2017

Supporting Information

Highly efficient hydrogen evolution electrocatalysts based on coupled molybdenum phosphide and reduced graphene oxide derived from MOFs

Ji-Sen Li,[a,b] Jing-Quan Sha,[b] Bing Du,[b] and Bo Tang*[a]

[a]College of Chemistry, Chemical Engineering and Materials Science, Collaborative Innovation Center of Functionalized Probes for Chemical Imaging in Universities of Shandong, Key Laboratory of Molecular and Nano Probes, Ministry of Education, Shandong Provincial Key Laboratory of Clean Production of Fine Chemicals, Shandong Normal University, Shandong 250014, China

[b]Key Laboratory of Inorganic Chemistry in Universities of Shandong, Department of Chemistry and Chemical Engineering, Jining University, Shandong, 273155, China

* E-mail: tangb@sdnu.edu.cn.

S1. Materials and preparation of the catalysts

Reagents and Chemicals.

Molybdenum trioxide (MoO_3), imidazole, and diammonium hydrogen phosphate ($(NH_4)_2HPO_4$) were purchased from Sinopharm Chemical Reagent Co. Ltd. Pt/C catalyst (20 wt% Pt/C) was purchased from Johnson Matthey. Nafion (5.0 wt%) was purchased from Sigma-Aldrich. All chemicals were used without further purification. The water used in the experiments was ultra-purified water (18.25 MΩ).

Synthesis of Mo-MOFs.

According to the previously reported literature,[1] Mo-MOFs were synthesized. Namely, 24.4 mmol of imidazole and 24.3 mmol MoO_3 were added into 250 mL of ultra-purified water. After the mixture was refluxed for 12 h, the sediment was collected by centrifugation. And then, washing with ultra-purified water and drying at vacuum at 70 ^{o}C, the Mo-MOFs were obtained.

Synthesis of MoO_2@NC/rGO and MoO_2@NC.

Graphene oxide (GO) was synthesized by the modified Hummer method.[2] 10 mg of Mo-MOFs were mixed with GO aqueous solution (2 mL, 1.3 mg mL^{-1}) and stirred for 4 h. Subsequently, the mixture was centrifuged at 2000 rpm for 3 min and washed with water several times. After freeze dyring, the white powder was obtained (designed as Mo-MOFs/GO) and heated at 600 ^{o}C for 3 h at a heating rate of 3 ^{o}C min^{-1} under Ar atmosphere (denote as MoO_2@NC/rGO).

The MoO_2@NC was synthesized by the same method as that for MoO_2@NC/rGO without adding the GO solution.

Synthesis of MoP@NPC/rGO and MoP@NPC

The mixture of MoO_2@NC/rGO (100 mg) and $(NH_4)_2HPO_4$ (500 mg) was grinded to powders and placed in a boat. Subsequently, the boat was heatd at different temperatures (750, 850, and 950 ^{o}C) for 2 h at a heating rate of 5 ^{o}C min^{-1} under H_2/Ar (10%/90% in volume rate), respectively. After cooling naturally at room temperature, the obtained sample denoted as MoP@NPC/rGO, MoP@NPC/rGO-850 and 950, respectively.

For comparison, the MoP@NPC was synthesized by the above procedures similar to that for MoP@NPC/rGO, but using MoO_2@NC as raw material.

Characterizations

The transmission electron microscopy (TEM) and high-resolution TEM (HRTEM) images were recorded on JEOL-2100F apparatus at an accelerating voltage of 200 kV. Surface morphologies of the carbon materials were examined by a scanning electron microscope (SEM, JSM-7600F) at an acceleration voltage of 10 kV. The powder X-Ray diffraction (PXRD) patterns were recorded on a D/max 2500VL/PC diffractometer (Japan) equipped with graphite monochromatized Cu Kα radiation (λ = 1.54060 Å). Corresponding work voltage and current is 40 kV and 100 mA, respectively. Inductively coupled plasma (ICP) measurements were performed on a Jarrel-Ash 1100 + 2000 Quantometer. X-ray photon spectroscopy (XPS) was recorded by a scanning X-ray microprobe (PHI 5000 Verasa, ULAC-PHI, Inc.) using Al kα radiation and the C1s peak at 284.8 eV as internal standard. The Raman spectra of dried samples were obtained on Lab-RAM HR800 with excitation by an argon ion laser (514.5 nm).

Electrochemical Measurements

All electrochemical experiments were conducted on a CHI 760D electrochemical station (Shanghai Chenhua Co., China) in a standard three electrode cell in 0.5 M H_2SO_4 solution at room temperature. A glassy carbon electrode (GCE, 3 mm in diameter), a saturated calomel electrode (SCE), and a graphite rode were used as the working electrode, reference and counter electrode, respectively. 4 mg of the catalysts were dispersed in 2 mL of 9:1 v/v water/Nafion by sonication to form a homogeneous ink. Typically, 5 μL well-dispersed catalysts were covered on the glassy carbon electrode and then dried in an ambient environment for measurements. The electrocatalyst was prepared with a catalyst loading of 0.14 mg cm^{-2}. Commercial 20% Pt/C catalyst was also used as a reference sample. A flow of N_2 was maintained over the electrolyte during the experiment to eliminate dissolved oxygen. The potential *vs* RHE was converted to the reversible hydrogen electrode (RHE) *via* the Nernst equation: $E_{\mathrm{RHE}} = E_{\mathrm{SCE}} + 0.059\ \mathrm{pH} + E^{\theta}_{\mathrm{SCE}}$. In 0.5 M H_2SO_4, $E_{\mathrm{RHE}} = 0.241\ \mathrm{V} + E_{\mathrm{SCE}}$.

Linear sweep voltammetry (LSV) was tested with a scan rate of 2 mV s^{-1}. Stability of the catalyst was conducted by cycling the potential between -0.2 to 0.14 V (*vs* RHE) at a scan rate of 100 mV s^{-1}. The chronoamperometry (CA) were tested at an overpotential of 218 mV (*vs* RHE). To estimate the electrochemical active surface areas of the catalysts, cyclic voltammogram (CV) was tested by measuring double-layer capacitance (EDLC) under the potential window of -0.059

to 0.041V (*vs* RHE) with various scan rate (from 20 to 200 mV s^{-1}).

S2. Figures in Supporting Information

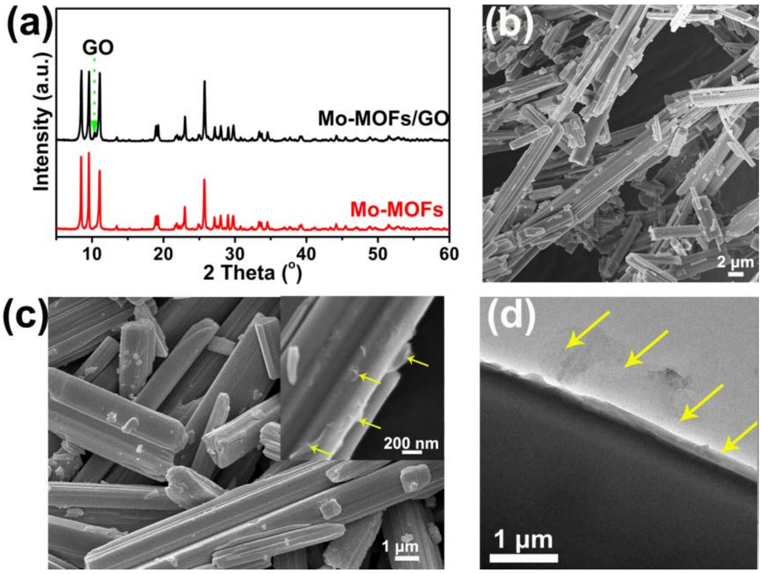

Fig. S1 (a) PXRD patterns of Mo-MOFs/GO (black) and Mo-MOFs (red). (b-c) SEM images of Mo-MOFs, and Mo-MOFs/GO. Inset in (c): Magnified SEM image of Mo-MOFs/GO. (d) TEM image of Mo-MOFs/GO. The yellow arrows exhibit GO.

As shown in **Fig. S1a**, the powder X-ray diffraction (PXRD) pattern of Mo-MOFs/GO is almost consistent with that of Mo-MOFs, confirming that the synthetic process of Mo-MOFs was not disturbed by the introduction of GO. Additionally, it is worth noting that a small peak (green arrow) is at about 10.5^{o}, which attests that GO is successfully introduced into the Mo-MOFs/GO nanocomposite. In contrast to the smooth surface of Mo-MOFs (**Fig. S1b**), a transmission electron microscopy (TEM), and scanning electron microscope (SEM) images of Mo-MOFs/GO show that the surface of Mo-MOFs is decorated with a thin layer of GO (**Fig. S1c, d**).

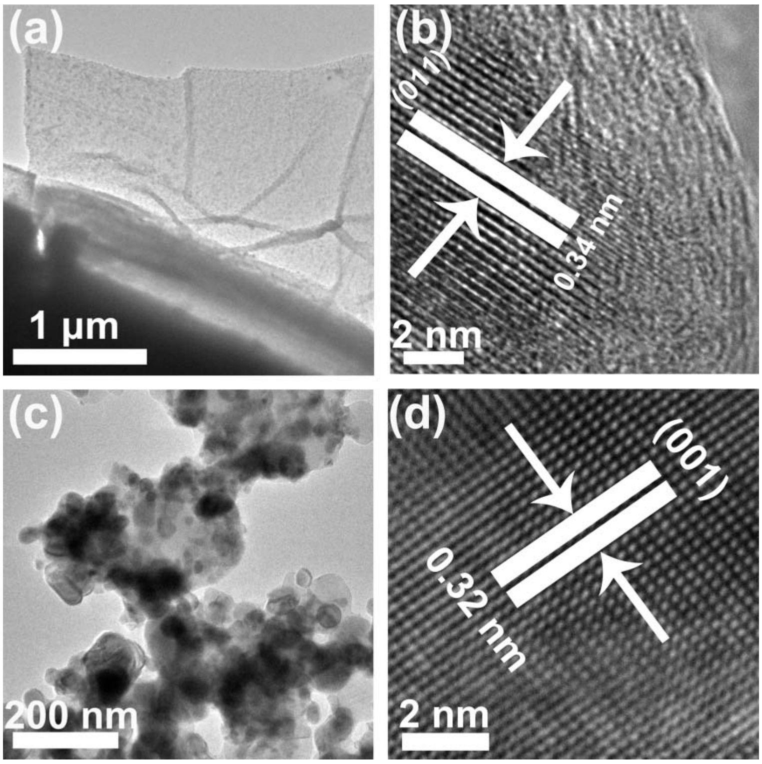

Fig. S2 TEM and HRTEM images of (a-b) MoO_2@NC/rGO and (c-d) MoP@NPC, respectively.

As indicated in **Fig. S2a**, the morphology of MoO_2@NC/rGO is similar to that of MoP@NPC/rGO. The HRTEM image (**Fig. S2b**) exhibits a lattice distance of 0.34 nm, assignable to the (011) plane of MoO_2. In term of MoP@NPC, only many irregular MoP NPs were obtained **(Fig. S2c, d)**, underlining that the introduction of GO is of critical importance to the fabrication process of MoP@NPC/rGO hybrid.

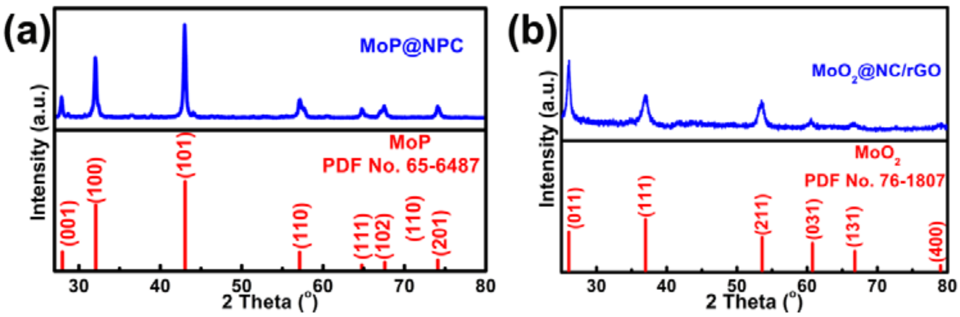

Fig. S3 PXRD patterns of MoP@NPC (a) and MoO$_2$@NC/rGO (b), respectively.

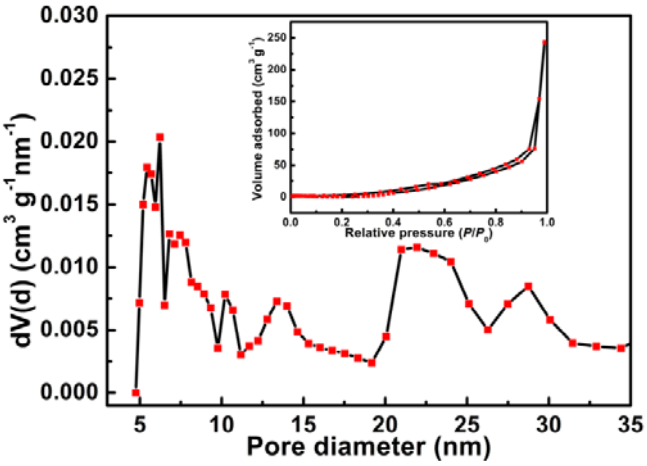

Fig. S4 The pore size distribution of MoP@NPC/rGO from DFT method. Inset: N_2 adsorption-desorption isotherm of MoP@NPC/rGO.

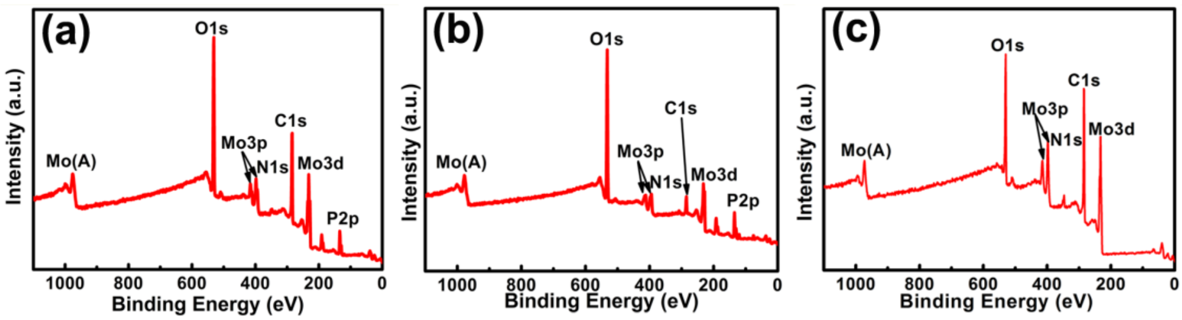

Fig. S5 (a-c) XPS survey spectra of MoP@NC/rGO, MoP@NPC, and MoO$_2$@NC/rGO, respectively.

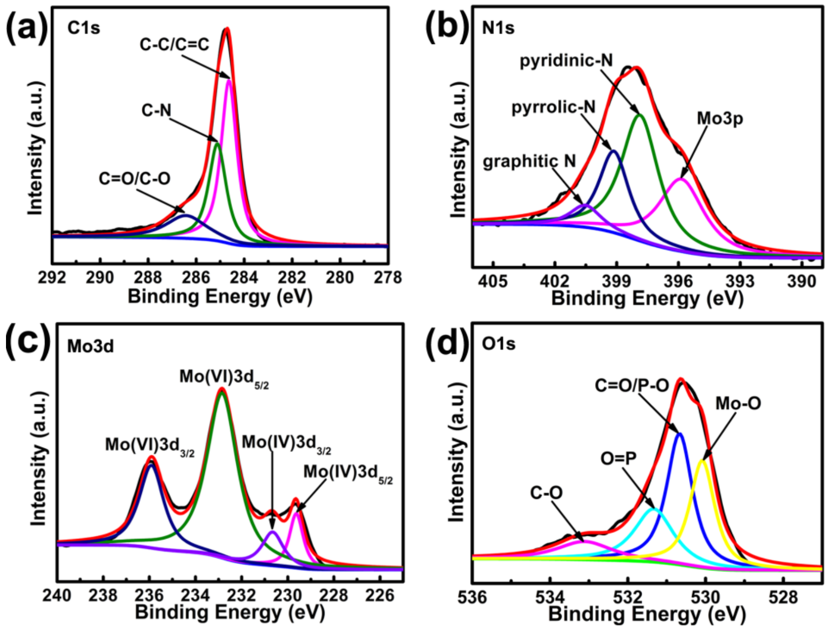

Fig. S6 High resolution XPS spectra of (a) C 1s, (b) N 1s, (c) Mo 3d, and (d) O1s of MoO_2@NC/rGO, respectively.

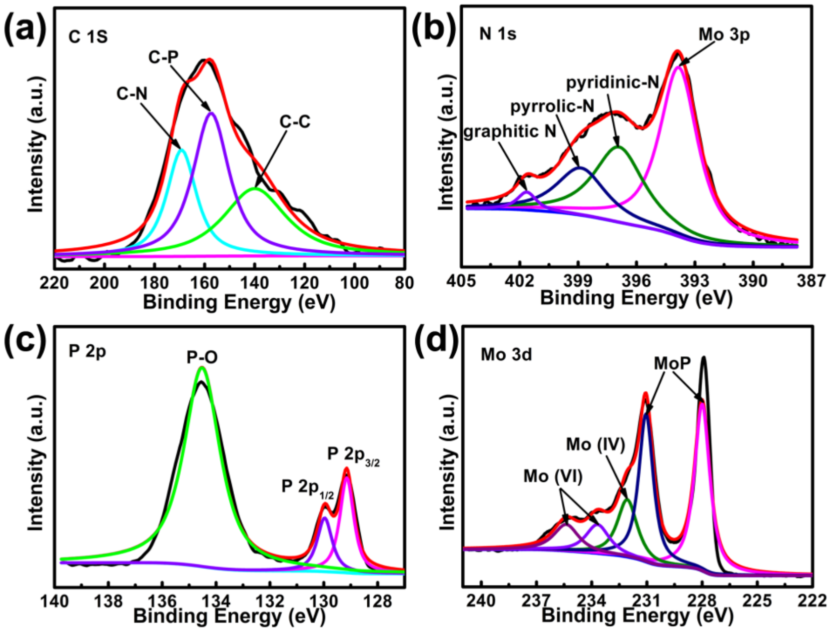

Fig. S7 High resolution XPS spectra of (a) C 1s, (b) N 1s, (c) P 2p, and (d) Mo 3d of MoP@NPC, respectively.

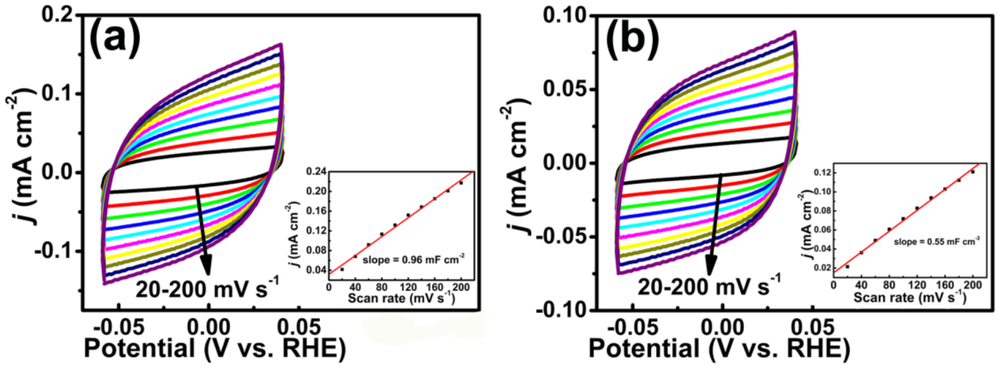

Fig. S8 (a-b) The CVs of MoO_2@NC/rGO and MoP@NPC with different rates from 20 to 200 mV s^{-1}, respectively. Inset: the capacitive current at - 0.009 V as a function of scan rate for MoO_2@NC/rGO and MoP@NPC, respectively.

ECSA and TOF calculation:

The electrochemical active surface area (ECSA) can be calculated according to the capacitance (C). Generally, the specific capacitance for a flat surface is found to be in the range of 20~60 μF cm^{-2}. 40 μF cm^{-2} was used in the following calculations of the ECSA and turnover frequency (TOF) as literatures generally did.[3,4]

The following formula was applied to estimate ECSA:

$$\text{ECSA} = \frac{\text{C}}{40\ \mu\text{F cm}^{-2}\ \text{per cm}^{-2}}$$

To estimate the TOF, we used the following formula:

$$\text{TOF} = \frac{\text{number of total hydrogen turnover per cm}^2}{\text{number of active site per cm}^2}$$

The total number of hydrogen turnovers was calculated from the current density according to the formula:[5]

$$\text{no. of H}_2 = (j\frac{\text{mA}}{\text{cm}^2})(\frac{1\,\text{C s}^{-1}}{1000\,\text{mA}})(\frac{1\,\text{mol H}_2}{96485.3\,\text{C}})(\frac{1\,\text{mol H}_2}{2\,\text{mol of e}^{-1}})(\frac{6.02\times10^{23}\ \text{H}_2\ \text{moleculars}}{1\,\text{mol H}_2})$$

$$= 3.12\times10^{15}\ \frac{\text{H}_2/\text{s}}{\text{cm}^2}\ \text{per}\ \frac{\text{mA}}{\text{cm}^2}$$

The number of active sites per surface area was calculated on the basis of the crystal data as follows:

$$\text{Active sites}_{\text{MoP}} = \left(\frac{2 \text{ atom / unit cell}}{28.71\,\text{Å}^3 \text{ / unit cell}}\right)^{\frac{2}{3}} = 1.693 \times 10^{15} \times \text{atoms cm}^{-2}{}_{\text{real}}$$

$$\text{TOF} = \frac{(3.12 \times 10^{15} \, \frac{\text{H}_2/\text{s}}{\text{cm}^2} \text{ per } \frac{\text{mA}}{\text{cm}^2})}{\text{surface sites} \times \text{A}_{\text{ECSA}}} \times |\text{j}|$$

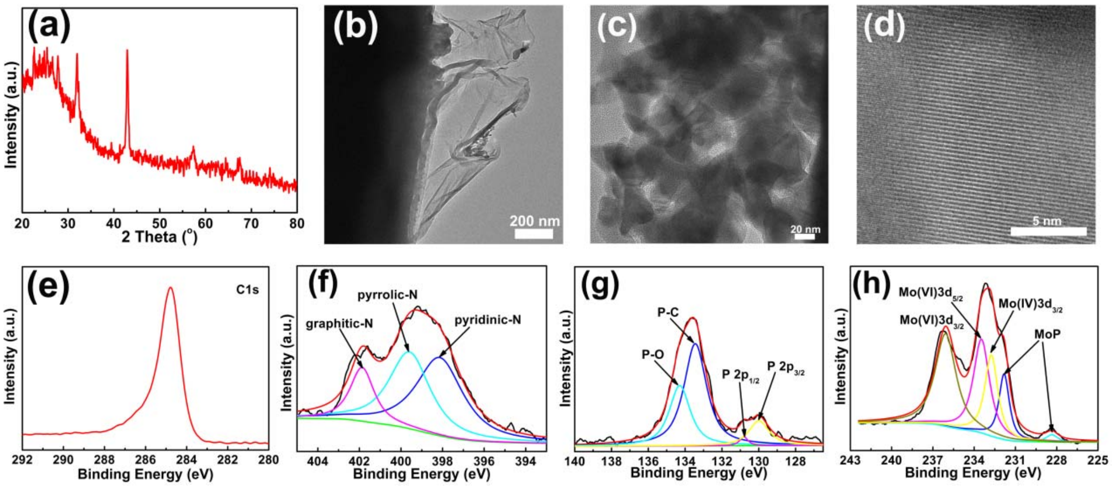

Fig. S9 (a) PXRD, (b-c) TEM, (d) HRTEM, (e-h) high resolution XPS spectra of C 1s, N 1s, P 2p, and Mo 3d of MoP@NPC/rGO after 1000 CV cycles, respectively.

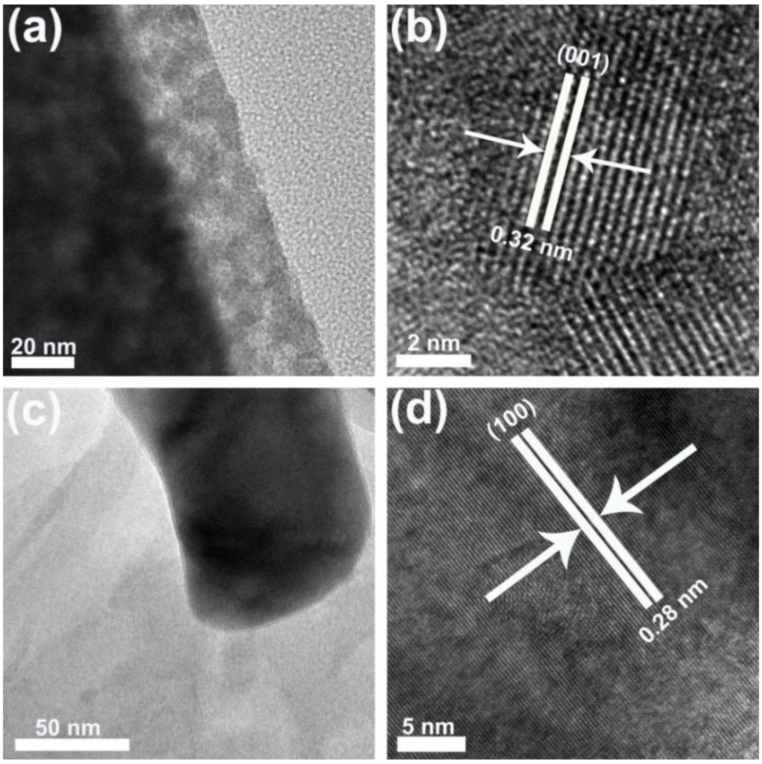

Fig. S10 TEM and HRTEM images of (a-b) MoP@NPC/rGO-850 and (c-d) MoP@NPC/rGO-950, respectively.

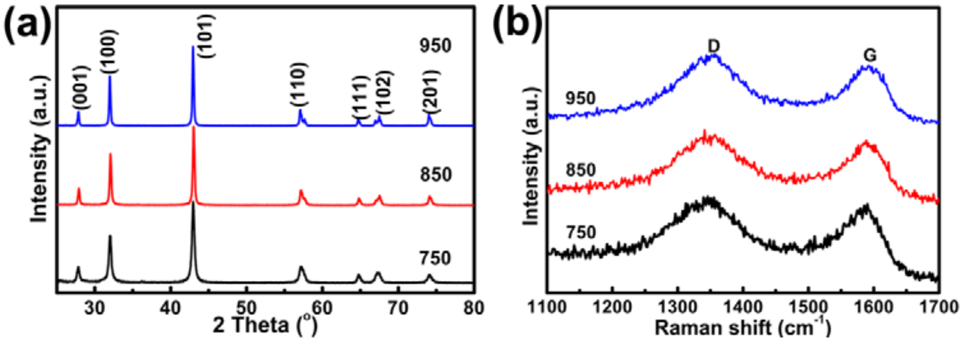

Fig. S11 (a-b) PXRD patterns and Raman spectra of MoP@NPC/rGO at different phosphidation temperature (750, 850, and 950 ^{o}C), respectively.

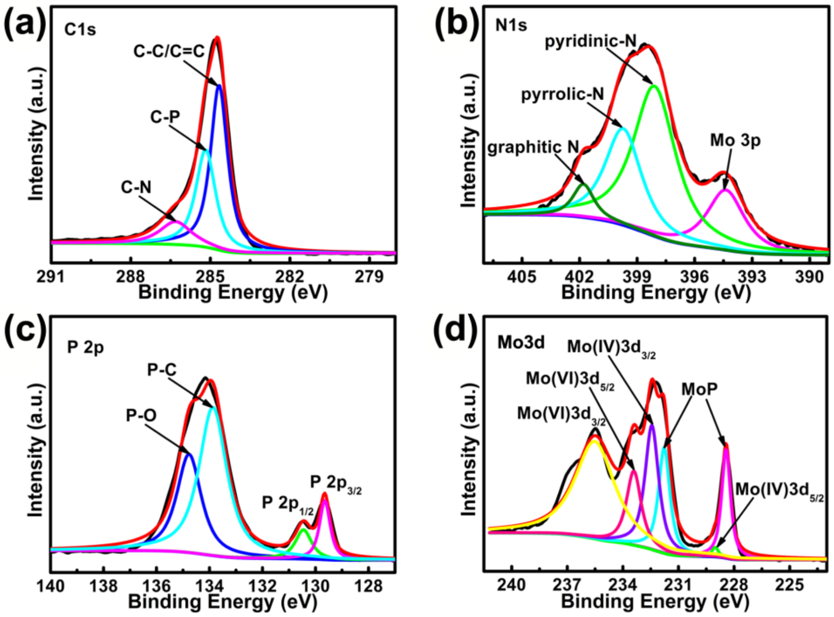

Fig. S12 High resolution XPS spectra of (a) C 1s, (b) N 1s, (c) P 2p, and (d) Mo 3d of MoP@NPC/rGO-850, respectively.

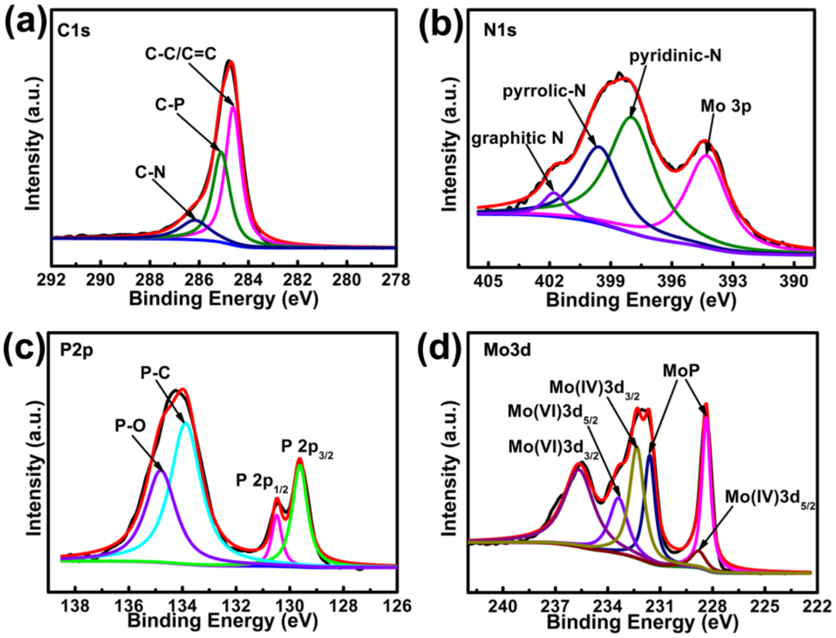

Fig. S13 High resolution XPS spectra of (a) C 1s, (b) N 1s, (c) P 2p, and (d) Mo 3d of MoP@NPC/rGO-950, respectively.

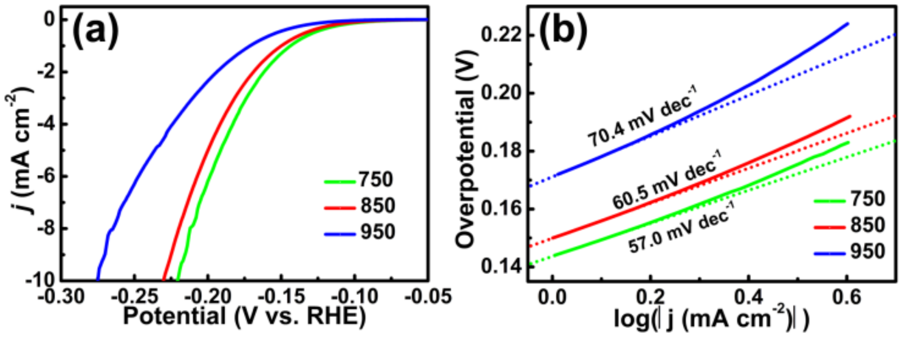

Fig. S14 (a) Polarization curves and (b) Tafe plots of MoP@NPC/rGO at different phosphidation temperature.

MoP@NPC/rGO-850, and MoP@NPC/rGO-950 were synthesized by a similar procedure, except for the phosphidation temperature being changed to 850 °C, and 950 °C, respectively. The corresponding morphology, structure and composition of the two catalysts were studied in detail **(Fig. S10-13)**. Simultaneously, the catalytic activities of the two samples towards the HER were also measured. Compared to MoP@NPC/rGO-850, and MoP@NPC/rGO-950, the MoP@NPC/rGO hybrid displays the lowest onset overpotential and the smallest Tafel slope in **Fig. S14**. Hence, 750 °C was selected as the optimal phosphidation temperature in this work.

S3. Table in Supporting Information

Table S1. Comparison of electrocatalytic performance of MoP-based HER catalysts.

Catalyst	Onset overpotential [mV][a]	Tafel slope [mV dec^{-1}]	η_{10} [mV][a]	Reference
MoP@NPC/rGO	**66**	**57**	**218**	**This work**
MoP	~110	75	~170	*J. Mater. Chem. A,* 2017, 5, 7191
MoP-C	67	82	135	*Nano Energy,* 2017, 32, 511
MoP/SN-650	44	46	104	*ACS Catal.*, 2017, 7, 3030
MoP	~120	66	240	*Adv. Mater.*, 2016, 28, 1427
MoP@PC	77	66	153	*Angew. Chem. Int. Ed.*, 2016, 128, 13046
MoP/CC	~106	52	*	*Energy Environ. Sci.*, 2016, 9, 1468
3D MoP	*	126	105	*J. Mater. Chem. A,* 2016, 4, 59
MoP NPs@NC	*	65	115	*Nanoscale,*2016, 8, 17256
MoP	~150	60	308	*Appl. Catal. A Gen*, 2016, 524, 134
MoP/rGO	16	58	119	*Chem. Commun.,*2016, 52, 9530
MoP/CF	*	56.4	199	*Appl. Catal. B,* 2015, 164, 144
MoP	50	54	150	*Energy Environ. Sci.,*2014, 7,2624–2629
MoP	100	60	246	*Chem. Commun.*, 2014, 50, 11683
MoP-CA2	40	54	125	*Adv. Mater.*, 2014, 26, 5702
MoP	*	50	117	*Angew. Chem. Int. Ed.* 2014, 53, 14433

[a] represents the overpotential (η) at the current density of 10 mA cm^{-2}. The potential measured versus RHE.

References

[1] P. Martian-Zarza, J. M. Arrieta, M. C. Munoz-Roca and P. Gili, *J. Chem. Soc., Dalton Trans.* 1993, 1551-1557.

[2] J. H. Lee, N. Park, B. G. Kim, D. S. Jung, K. Im, J. Hur and J. W. Choi, *ACS Nano*, 2013, **7**, 9366-9374.

[3] D. C. Grahame, *Chem. Rev.*, 1947, **41**, 441-501.

[4] X.-D. Wang, H.-Y. Chen, Y.-F. Xu, J.-F. Liao, B.-X. Chen, H.-S. Rao, D.-B. Kuang and C.-Y. Su, *J. Mater. Chem. A*, 2017, **5**, 7191-7199.

[5] J. Kibsgaard and T. F. Jaramillo, *Angew. Chem. Int. Ed.*, 2014, **53**, 14433-14437